analytical chemistry

Article

pubs.acs.org/ac

High-Throughput Microfluidic Single-Cell Digital Polymerase Chain Reaction

A. K. White,[†] K. A. Heyries,[†] C. Doolin,[‡] M. VanInsberghe,[†] and C. L. Hansen*[,†,‡]

[†]Centre for High Throughput Biology and [‡]Department of Physics and Astronomy, University of British Columbia, 307-2125 East Mall, Vancouver, British Columbia, Canada V6T 1Z4

Supporting Information

ABSTRACT: Here we present an integrated microfluidic device for the high-throughput digital polymerase chain reaction (dPCR) analysis of single cells. This device allows for the parallel processing of single cells and executes all steps of analysis, including cell capture, washing, lysis, reverse transcription, and dPCR analysis. The cDNA from each single cell is distributed into a dedicated dPCR array consisting of 1020 chambers, each having a volume of 25 pL, using surface-tension-based sample partitioning. The high density of this dPCR format (118 900 chambers/cm^2) allows the analysis of 200 single cells per run, for a total of 204 000 PCR reactions using a device footprint of 10 cm^2. Experiments using RNA dilutions show this device achieves shot-noise-limited performance in quantifying single molecules, with a dynamic range of 10^4. We performed over 1200 single-cell measurements, demonstrating the use of this platform in the absolute quantification of both high- and low-abundance mRNA transcripts, as well as micro-RNAs that are not easily measured using alternative hybridization methods. We further apply the specificity and sensitivity of single-cell dPCR to performing measurements of RNA editing events in single cells. High-throughput dPCR provides a new tool in the arsenal of single-cell analysis methods, with a unique combination of speed, precision, sensitivity, and specificity. We anticipate this approach will enable new studies where high-performance single-cell measurements are essential, including the analysis of transcriptional noise, allelic imbalance, and RNA processing.

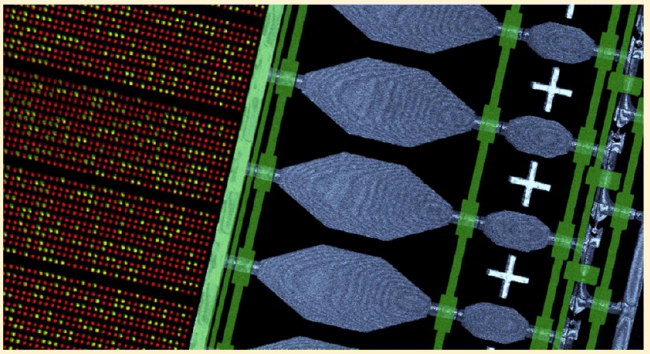

Cells are the fundamental unit of biology. Despite this, the vast majority of gene expression measurements have been performed using bulk samples of RNA extracted from large populations of cells having undefined composition and heterogeneity. Underlying the interpretation of such data is the assumption that all cells are similar and that the ensemble average of many individuals accurately captures the biology. Unfortunately, this assumption is often false. Significant cellular heterogeneity exists in most samples and is manifest at multiple levels, including the epigenetic[1,2] and transcriptional[3] states, protein expression,[4] and post-translational modifications, growth characteristics,[5] and functional responses.[6] Population measurements generally obscure this heterogeneity and muddy the biological interpretation: existing protocols for the isolation of rare stem cell populations typically provide functional purities between 1% and 50%,[7−9] resulting in significant and often overwhelming contamination from undefined subpopulations; the analysis of gene expression responses can be blurred by cellular asynchrony,[10] and many fundamental biological questions, including the degree to which cells regulate mRNA expression and processing, require measurements at the single-cell level.

The development of methods to measure and understand cellular variability has reached the point of "mission critical" and stands to impact a wide array of fundamental and applied fields ranging from immunology to regenerative medicine to microbiology. In response to this need, an expanding array of single-cell genomics methods are being advanced, each appropriate to different levels of inquiry. The coupling of whole transcriptome RNA amplification with high-throughput sequencing is now an established method for global analysis of single-cell expression profiles.[11] Although there still remain issues of representational bias, technical noise, and sequencing cost, the continued development of improved instrumentation, bioinformatics approaches, and optimized reagent kits[12] is likely to bring single-cell whole transcriptome amplification (WTA) analysis into the mainstream. Reverse transcription quantitative polymerase chain reaction (RT-qPCR), in either the conventional[13,14] or microfluidic[15,16] format, is perhaps the most versatile method for single-cell gene expression analysis.[17] Although well-suited to identifying and monitoring cellular subpopulations using established panels of genes,[18−20] RT-qPCR does not provide absolute measurements and has limited precision and specificity when working with low-abundance templates. These limitations make RT-qPCR suboptimal for

Received: March 26, 2013
Accepted: July 1, 2013
Published: July 2, 2013

 © 2013 American Chemical Society

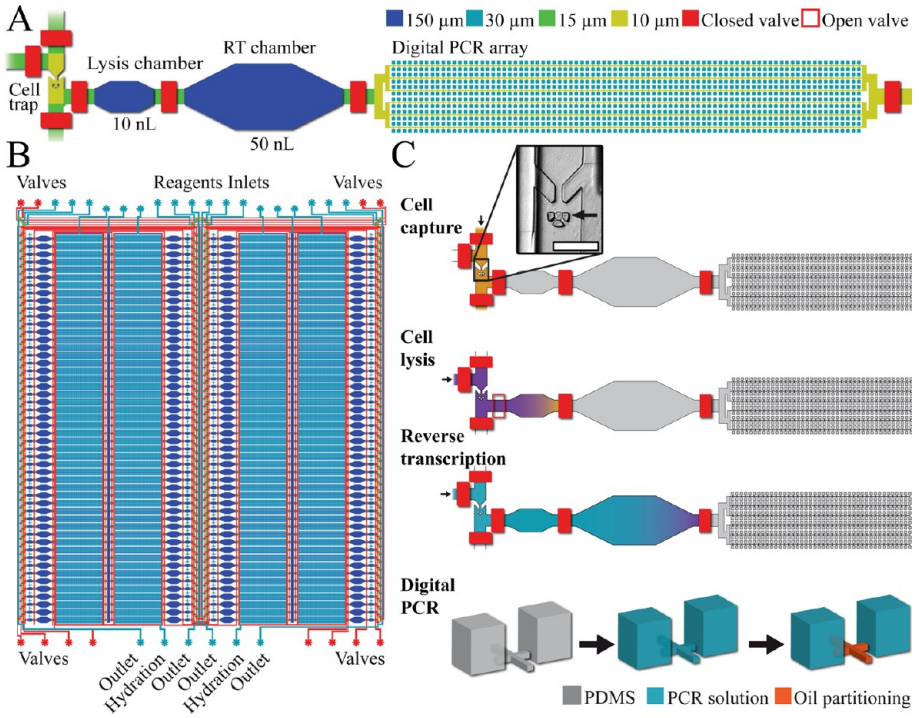

Figure 1. Microfluidic device design and operation. (A) Layout of the microfluidic modules for single-cell digital PCR analysis. The cells are trapped and lysed, and the transcript target is reverse transcribed before being injected into a digital PCR array. The respective height dimensions for the chambers and channels are indicated. (B) Complete microfluidic device. Four main panels contain 50 identical modules capable of parallel processing of up to 200 single cells. The device also contains a network of hydration channels to prevent water loss during thermocycling. (C) Workflow schematic for single-cell digital PCR analysis of mRNA. Depending on the protocol used for mRNA or miRNA analysis, cells are either chemically or heat lysed after being trapped (inset, K562 cells trapped; the scale bar is 100 μm). Transcripts are then reverse transcribed to cDNA by mixing RT reagents using diffusion. PCR reagents are then injected into the device, mixed by diffusion with cDNA products, and injected into the digital PCR array using dead-end filling. A fluorinated oil (FC-40) is then used to displace the remaining PCR solution in the channels and compartmentalize individual PCR digital chambers.

applications that require high-performance measurements of a small number of targets, including studies of transcriptional noise or allelic imbalance, single-cell genotyping, and the absolute quantitative analysis of low-copy transcripts.

For such demanding applications two single-molecule counting methods have emerged: mRNA fluorescence in situ hybridization (mRNA FISH)[21,22] and digital polymerase chain reaction (dPCR).[23] mRNA FISH has the important advantage of preserving spatial information regarding the location of cells within a tissue and has been applied to whole organisms. However, this method requires a lengthy sample preparation protocol, a complex probe design, and the need for sophisticated image acquisition and analysis steps. In addition, although mRNA FISH can in principle provide absolute transcript numbers, in practice this is often limited by difficulty in resolving closely localized fluorescent spots, interference from background fluorescence, ambiguity in defining cellular boundaries, and a broad distribution of intensities from hybridization events. More fundamentally, the need for multiple hybridization probes makes mRNA FISH poorly suited to measurements of small RNA species or discrimination of transcripts with high sequence homology.[21]

The alternative approach, dPCR, uses compartmentalization of single molecules at limiting dilution followed by PCR amplification and end-point detection to enable precise and highly specific quantification of transcripts. Although this approach has been used to make precise measurements of single-cell transcription,[23] throughput is typically restricted by the labor and cost of cell isolation and processing in conventional microliter volumes, as well as limitations in the throughput of dPCR analysis. Microfluidic systems can address these issues by providing economy of scale, automation, and parallelization, as well as increased reproducibility and sensitivity in small-volume reactions.[24] We previously developed a microfluidic device that implements integrated RT-qPCR at a throughput of 300 single cells per run.[10] This device performs steps of cell lysis, RT, and PCR by sequentially transferring reagents through three chambers, ending with PCR amplification of each cell product in single 50 nL chambers. A related device, featuring additional cell processing chambers and sample elution capabilities, has recently been released as a commercial product (Fluidigm C1). In separate work we have also developed a dPCR format that uses surface tension partitioning to achieve planar dPCR densities up to 400 000 chambers/cm^2.[25] Here we combine the advantages of integrated single-cell processing[10] and high-density dPCR[25] to enable high-throughput single-cell dPCR. Our device is capable of processing 200 single cells per run, each of which is analyzed in an array of 1020 PCR reactions, each having a volume of 25 pL, for a total of 204 000 PCR reactions per experiment. We establish the technical performance of this system using RNA dilutions and demonstrate its use in making absolute single-cell measurements of the expression of high-abundance (GAPDH) and low-abundance (BCR-ABL) transcripts, as well as the abundance of a mature micro-RNA (miR-16). Finally, we apply our system to the measurement and single-nucleotide discrimination of RNA editing of EEF2K transcripts in single cells.

dx.doi.org/10.1021/ac400896j | *Anal. Chem.* 2013, 85, 7182−7190

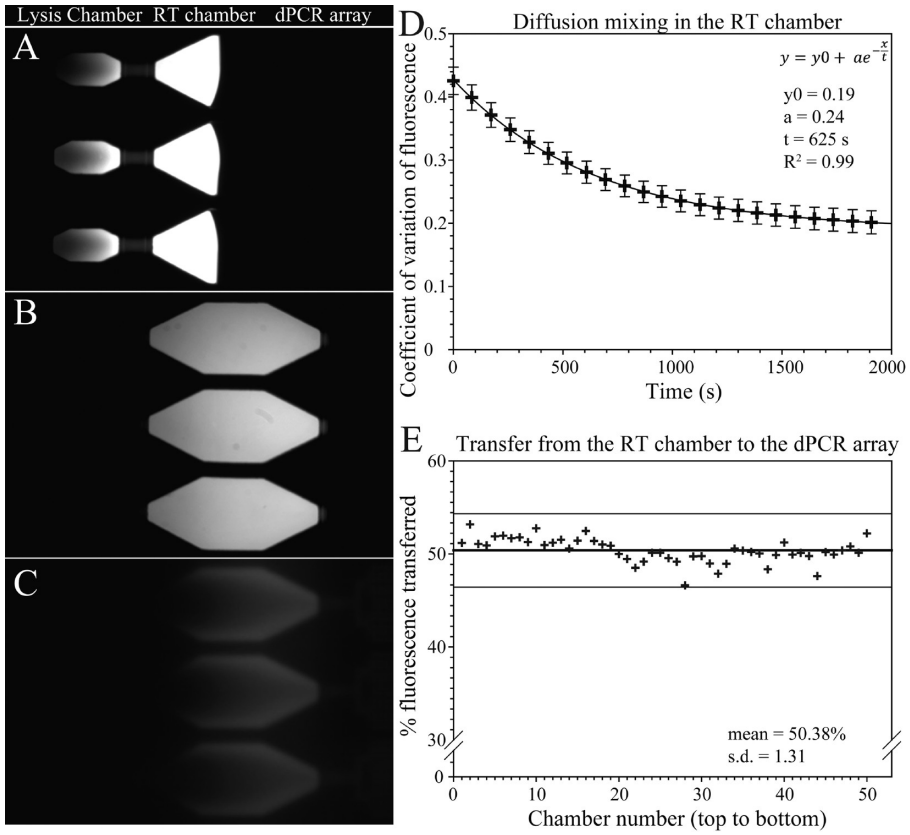

Figure 2. Characterization of the microfluidic device. (A) A solution containing 40 base oligonucleotides labeled with FAM was injected into the lysis chamber following the normal procedure. A second solution (not fluorescent) was then used to sequentially push the first solution into the RT chamber (B) and then the dPCR array (C). (D) Mixing by diffusion in the RT chamber (B) was monitored by measuring the standard deviation of the fluorescent signal over time. As expected, the signal follows an exponential decay with an averaged time constant (t) of 625 s (R^2 = 0.9999, N = 50). (E) To measure the amount of the cell sampled by the dPCR array, the fluorescent solution in the RT chamber was pushed into the digital PCR array using a nonfluorescent solution (C). The transfer efficiency was evaluated for 50 chambers and found to be 50.38% (SD = 1.31). The $\pm 3\sigma$ ranges from the mean lines are also displayed.

MATERIALS AND METHODS: MICROFLUIDIC SINGLE-CELL DIGITAL PCR DEVICE DESIGN AND OPERATION

The microfluidic device presented here consists of 200 identical modules (Figure 1A) divided into 4 linear arrays. Each array contains 50 modules (Figure 1B) with 3 chambers connected in series, followed by a dPCR array. This architecture allows for the implementation of a three-step protocol that requires sequential additions of reagents without purification, followed by dPCR analysis of the resulting products. Examples of two such protocols, one for mRNA quantification and one for miRNA quantification, can be performed as shown in Figure 1C (see the Supporting Information for the protocol details). Cells are first trapped in the "cell capture chamber" (0.8 nL) using hydrodynamic traps[10] and are then washed with fresh phosphate-buffered saline (PBS). Reagents are then introduced through the cell capture chamber to fill the subsequent "cell lysis chamber" (10 nL) and the "RT chamber" (50 nL). Finally, half of the product from each RT chamber is loaded into an independent dPCR array having 1020 chambers, sufficient to accurately measure the mRNA and miRNA targets ranging from approximately 3 to 5000 copies per cell. Further details of the device fabrication and operation can be found in the Supporting Information.

RESULTS

Device Performance. We first characterized the efficiency and uniformity of mixing and sample transfer in our microfluidic device using FAM-labeled 40 bp oligonucleotides. Sample transfer between the cell lysis chamber and RT chamber, as measured by fluorescence quantification, was found to be better than 99%; the amount of oligonucleotide remaining in the 10 nL chamber was below 1%, which is determined as the limit of detection for this measurement based on 2 standard deviations from the measured background fluorescence (Figure 2A). We next assessed the mixing of reagents in the 50 nL chamber by taking time lapse images of the fluorescence and calculating the variability in oligonucleotide concentration across the chambers. Regression of the resulting data to an exponential decay curve yielded a mixing time constant of approximately 11 min (Figure 2D). On the basis of this analysis, we implemented a 30 min wait time in our protocol to allow for sufficient reaction mixing. Finally, we measured the reproducibility of transfer from the RT chamber to the digital PCR array. Fluorescence measurements of the 50 nL chamber before and after injection into the dPCR array showed that the fraction of solution that was injected into the digital PCR array was 50.38% (SD = 1.31%) (Figure 2E).

We next performed a series of experiments to assess the signal-to-noise and measurement sensitivity of our system using a total RNA template purified from K562 cells. Using hydrolysis

dx.doi.org/10.1021/ac400896j | Anal. Chem. 2013, 85, 7182−7190

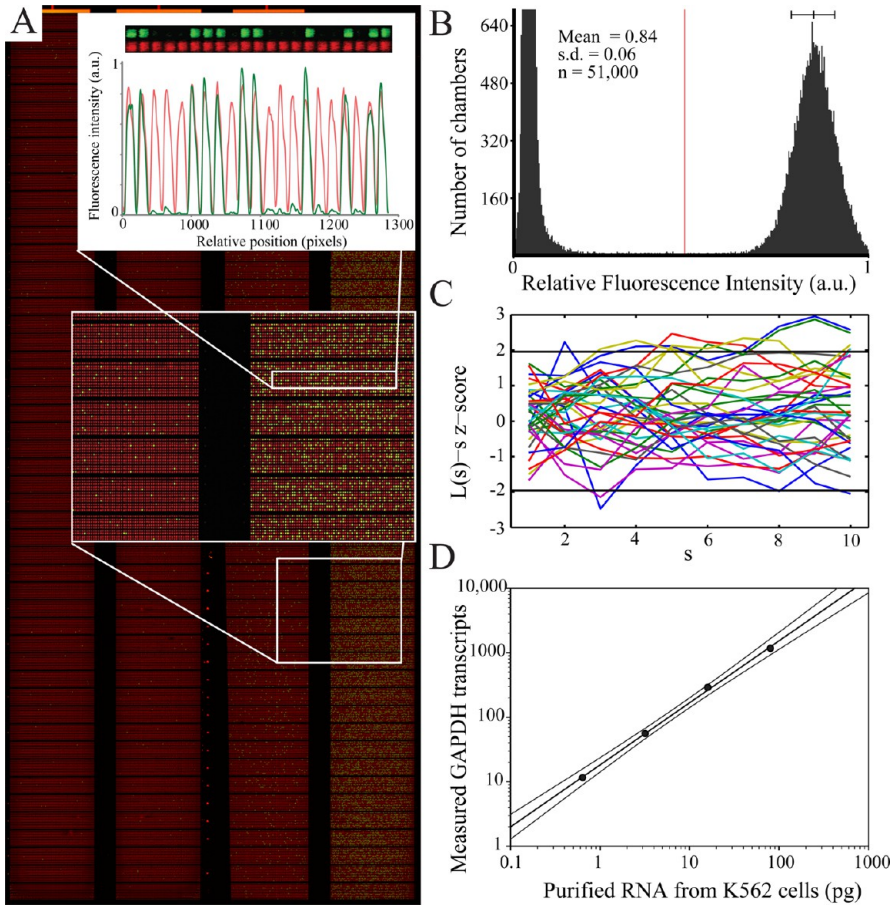

Figure 3. Digital PCR measurements. (A) End point fluorescence signal from the entire microfluidic device after dPCR targeting GAPDH. RNA dilutions have been loaded into four different visible panels and reverse transcribed on chip. The resulting cDNA is quantified by digital PCR where digital PCR positive hits (green) in 30 pL chambers have a high signal-to-noise ratio (>30). A passive dye (red) is visible in all the chambers. (B) Histogram of the distribution fluorescence intensity for 51 000 digital PCR chambers with 20 pg of RNA as the starting material. The normalized mean and standard deviation of the bright, or positive, chambers are indicated. (C) Randomness of the distribution of detected transcripts within a distance *s* in the dPCR array assessed by using *z*-scores of a variance-stabilized Ripley *k*-function (*L*-function) within a 95% confidence interval. (D) Dynamic range of the digital PCR arrays using 5-fold serial dilutions of total RNA purified from K562 cells, looking at GAPDH mRNA. Linear regression analysis using the experimental data was performed (parameters displayed with 95% confidence boundaries).

probes (TaqMan), the signal-to-noise ratio obtained using the four different assays allowed a clear and unambiguous discrimination between the positive and negative chambers (Figure 3A). Figure 3B shows a histogram of fluorescent intensities, with a signal-to-noise ratio in excess of 30, obtained across 51 000 fluorescent chambers in one lane of the device measuring GAPDH transcripts (part A, inset, and part B of Figure 3).

Digital PCR requires template molecules to be randomly distributed among reaction chambers to accurately infer the number of molecules in the array from the number of reaction chambers with PCR amplification. Our integrated single-cell dPCR device mixes PCR solution with template by diffusion in 50 nL chambers prior to injection into the array of 1020 × 25 pL dPCR chambers, having an aggregate array volume of approximately 25 nL. We assessed the randomness of the resulting distribution of cDNA molecules across the dPCR array by plotting the *z*-score of the variance-stabilized Ripley *k*-function[26,25] for 50 subarrays in a single lane of the device loaded with purified RNA at a concentration of ~18 pg per array (single-cell equivalent) (Figure 3C), with the RNA loaded through the cell processing chambers and subsequent processing performed in the same sequence as during single-cell analysis. This analysis shows that the distributions are not significantly different from random and lie within a 95% confidence interval constructed around the mean of 500 simulated data sets, based on a Poisson distribution of template molecules in each chamber.[27,26] This statistical analysis was also repeated for single-cell measurements and demonstrates that mRNA distributions are also within 95% confidence intervals under this scenario (Supplemental Figure 1, Supporting Information).

Finally, to verify the response and precision of the device, we measured the abundance of GAPDH mRNA from serial dilutions of total RNA purified from K562 cells (Figure 3D). Measured concentrations from 5-fold RNA dilutions were in excellent agreement with the expected template abundance and dilution factor (R^2 = 0.9989), with tested values spanning a chamber occupancy rate between 0.02% and 48% (Figure 3A), corresponding to a range of 80−0.64 pg of total RNA template per reaction.

Single-Cell Transcript Measurements. We then conducted a series of single-cell experiments to establish the combined capabilities of high-throughput cell processing and dPCR analysis. As a first test we performed measurements of GAPDH transcripts from single K562 cells (Figure 4A).

dx.doi.org/10.1021/ac400896j | *Anal. Chem.* 2013, 85, 7182−7190

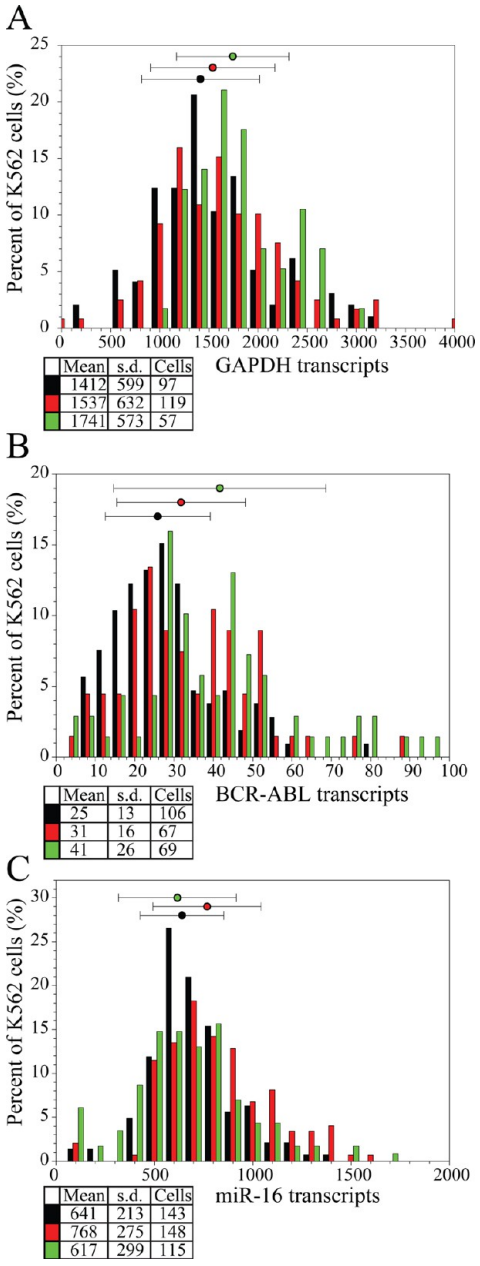

Figure 4. Digital PCR measurements on K562 single cells. (A) GAPDH mRNA transcript abundance measurements over three independent experiments. The transcript abundance frequency displayed on the *x*-axis is binned every 200 transcripts. (B) Micro-RNA miR-16 measurements over three independent experiments. The transcript abundance frequency displayed on the *x*-axis is binned every 100 transcripts. (C) BCR-ABL fusion gene mRNA transcript measurement over three independent experiments. The transcript abundance frequency displayed on the *x*-axis is binned every four transcripts.

GAPDH encodes for glyceraldehyde 3-phosphate dehydrogenase and is a commonly used high-copy-number endogenous control for RT-qPCR experiments.[23,10,28] Over a total of three device runs, we observed successful amplification for 100% of the isolated single cells (N = 288). We note that the total number of cells analyzed was lower than the theoretical device capacity due to the use of some device lanes for controls and suboptimal cell trapping efficiency; these experiments were performed with an unoptimized cell trap geometry that resulted in approximately 60% single-cell occupancy. Further trap optimization has resulted in 96% single-cell occupancy. However, reaction chambers that did not capture a cell provide stringent no-cell controls from which to evaluate the background signal in analysis. In these no-cell controls, we observed a very low frequency of mRNA detection events, with an average of 1.6 hits per no-cell chamber (N = 106 chambers), corresponding to background mRNA contamination levels below 0.1%. No correlation was observed between the background signal and the copy number measured on single cells in adjacent wells.

The measured number of transcripts in single cells revealed a log-normal distribution ($0.94 < R^2 < 0.98$) of GAPDH with an average copy number of 1563 transcripts per single cell. In three replicate measurements, performed on separate devices and different cultures, the mean GAPDH expression was very reproducible, ranging from 1412 to 1741 copies per cell. These values are in good agreement with estimates of 1761 (SD = 648) copies we have previously made by normalizing single-cell microfluidic RT-qPCR measurements to a standard curve calibrated by dPCR.[10] All replicates revealed a large variability in GAPDH expression between cells, with measured values spanning approximately 10-fold in absolute copy number (~400−4000 copies). This variability in GAPDH levels was also consistent between runs, with an average standard deviation of 601 ± 24 copies per cell.

To demonstrate the use of high-throughput digital PCR in accurate quantification of low-abundance transcripts, we next measured the expression of BCR-ABL transcripts, a fusion gene resulting from a reciprocal translocation of chromosomes 9 and 22 that is associated with chronic myelogenous leukemia (CML) and is also present in K562 cells. Over three runs we reliably detected the BCR-ABL fusion transcript in every cell analyzed (N = 242), with a mean expression of 33 copies per cell, a range spanning 25-fold in relative expression (4−100 copies per cell), and a standard deviation of 18.9 copies per cell (Figure 4B). These measurements were consistent with an independent study based on RT-qPCR[29] which measured BCR-ABL mRNA in single K562 cells ranging from 2 to 262 copies per cell, with the majority of cells containing approximately 40 copies per cell.

Using an alternative two-step RT-PCR protocol, we next demonstrated the use of our technology for absolute measurements of micro-RNA (miRNA) levels in single cells. miRNAs are a large family of conserved short (~22 base pairs) noncoding RNAs that associate into the RNA-induced silencing complex (RISC) and function as post-transcriptional regulators via targeted degradation of complementary transcripts or by repressing translation.[30] miRNAs are important regulators in many biological processes, including development, oncogenesis,[31] and immunity, making them of high interest as biomarkers of disease.[32] Due their short length, miRNAs are not easily amenable to single-molecule analysis by RNA FISH,[33] and although hybridization techniques have been used to visualize miRNAs,[34,35] single-molecule quantification of miRNA copy numbers and variability in single cells by FISH have not been achieved. Using a commercially available RT-qPCR detection strategy, based on miRNA-specific stem−loop reverse transcription primers,[18] we measured the expression and variability of miR-16, a micro-RNA expressed at medium levels across a broad range of tissues, in K562 cells. Over three replicates, K562 cells were found to have a mean copy number of 675 per cell, which is in close agreement with dPCR

dx.doi.org/10.1021/ac400896j | *Anal. Chem.* 2013, 85, 7182−7190

measurements performed on bulk samples.[10] The distribution of miR-16 expression was consistent across runs, with a standard deviation of 262 ± 44 (Figure 4C).

Finally, we applied our single-cell dPCR device to measure the extent of single-nucleotide RNA editing. Editing of RNA molecules by nucleoside deaminases has recently gained attention as a mechanism by which transcripts can be modified away from the genomic code, with potential implications for transcript stability, alternative splicing, translation efficiency, and protein sequence. Next-generation sequencing techniques have provided strong evidence for large numbers of RNA editing events across different tissues. These events are typically incomplete, representing a fraction of the total RNA. However, little is known regarding the variability of editing between individual cells. Is there a subset of cells that edit all transcripts? Is the frequency of editing similar across different cells? To investigate these questions, we used the specificity of dPCR to measure adenosine to inosine editing of position chr16:22296860 (hg19) in the mRNA coding for EEF2K in single cells. This edit was initially identified in a lobular breast cancer[36] and found to be edited at a frequency of ∼0.33 in RNA-seq data from ENCODE.[37] Wild-type and edited versions of EEF2K, differing by a single-nucleotide substitution, were simultaneously measured on single cells using a two-color TaqMan SNV assay based on minor groove binding probes (Life Technologies). We measured EEF2K in 221 single K562 cells and found 71 of 221 (32%) cells in which both wild-type and edited EEF2K transcripts were expressed, 12 of 221 (5%) cells in which only edited transcripts were expressed, 103 of 221 (47%) cells in which only wild-type transcripts were edited, and 35 of 221 (16%) cells in which neither form of EEF2K transcript was detected (Table 1). The population-averaged editing frequency was found to be ∼0.19 from single-cell measurements, which is consistent with our measurements on dilutions of purified RNA, producing an edit frequency of ∼0.18. We observed no nonspecific amplification in any no-cell reactions. A control experiment omitting the RT enzyme detected genomic wild-type EEF2K in 10 out of 228 single-cell reactions (∼4.4%) and no observed positives for the edited transcript.

Table 1. Measurement of Single-Nucleotide RNA Editing of EEF2K in Single K562 Cells[a]

WT EEF2K mRNA (copies) \ Edited EEF2K mRNA (copies)	0	1	2	3	
0	35 (16%)	10	2	0	12 (5%)
1	42	16	7	0	
2	20	12	4	0	
3	21	7	3	0	
4	10	8	3	1	
5	7	1	0	0	
6	0	7	0	0	
7+	3	0	2	0	
	103 (47%)				71 (32%)

[a]Single cells are binned according to the abundance of wild-type (WT) or edited EEF2K transcript. Quadrants containing homozygous wild-type, homozygous edited, heterozygous wild-type and edited, and not-detected EEF2K expression are indicated in color.

DISCUSSION AND CONCLUSION

Single-cell dPCR is particularly well suited to measurements that require high precision and sensitivity. We note that the half-sampling approach implemented here introduces additional stochastic variation in measured cDNA copy number that is particularly important for low-abundance transcripts. A theoretical analysis of the measurement precision of digital PCR has previously been presented.[38] Following this treatment, we calculated the expectation value, confidence intervals, and coefficient of variance for our 1020-chamber dPCR array as a function of the total number of molecules that are loaded into the array (assuming no losses for sampling). To generate confidence intervals that also include the effect of half-sampling, we implemented a Monte Carlo method. Briefly, a starting population of m molecules were uniformly and randomly assigned to two groups, n (sampled in the array) and o (not sampled in the array). Each n molecule was then uniformly and randomly assigned a detection chamber, allowing for the possibility of multiple molecules assigned to the same chamber. The number of chambers containing at least one molecule (k) was then counted and stored in association with the starting m. This process was repeated for $1 \leq m \leq 20\,400$ a total of 10 000 times each. These results were then searched for each value of k ($1 \leq k \leq 1020$) to generate distributions for the number of starting m molecules which led to k hits. The sample average, standard deviation, and 95% confidence intervals were then calculated from these distributions. On the basis of the results, summarized in Supplemental Figure 2 (Supporting Information), half-sampling is the dominant source of measurement error over the entire dynamic range of measurement (approximately 5 logs). Nevertheless, the aggregate precision is still excellent, with 93% of the potential 5-log dynamic range of the device having a coefficient of variance (CV) of less than 0.1 and 75% having a CV of less than 0.05. We further note that incomplete sampling of single-cell products is also a feature of previously reported single-cell dPCR.[23,39] This sampling variability could be reduced through improvements in device architecture and/or modified protocols, including preamplification prior to loading the dPCR array, pushing the sample into the array with an immiscible fluid to avoid dilution, or using sequential load and mix steps to assay dilutions of a single-cell product in multiple arrays. Finally, we note that dPCR experiments should be interpreted as measurements of the absolute cDNA molecule copy number, with the direct correlation to mRNA abundance dependent on the RT efficiency, which may vary between different assays.

Here we have demonstrated the application of our system in making absolute measurements of cDNA derived from mRNA and miRNA across hundreds of single cells. Measurements of GAPDH transcript levels, commonly used as an endogenous control in qPCR analysis, show that population-averaged expression measurements are consistent across different cultures, but are widely variable (CV ≈ 40%) at the single-cell level. This highlights how the common practice of normalizing single-cell RT-qPCR expression measurements to a "control gene" is not advisable and is likely to introduce additional noise. Our measurements also show that miR-16, widely used as an endogenous reference for miRNA analysis,[18] exhibits a similar coefficient of variation (CV ≈ 40%) at the single-cell level, although at approximately 2-fold lower expression. As a measure of variability, we calculate the Fanno factor, defined as $F = \sigma^2/\mu$, for GAPDH and miR-16 to be 231 and 102, respectively, showing that miR-16 is more tightly regulated in these cells. K562 cells are an inherently heterogeneous sample, and much of the measured variability in both GAPDH and miR-16 may represent differences in the differentiation state, cell cycle stage, and cell volume.

dx.doi.org/10.1021/ac400896j | Anal. Chem. 2013, 85, 7182−7190

In addition to the quantification of short transcripts such as miRNA, dPCR is uniquely suited to the detection and quantification of transcripts having high sequence homology. Here we have demonstrated this capability in studying the single-cell distribution of RNA editing events that give rise to a single-nucleotide variant in EEF2K. Given the low copy number of this transcript, it is difficult to conclude that the noise in EEF2K measurements represents a significant difference in editing between cells; we note that EEF2K was chosen as it was also found to be edited in other tissues (see the supplemental methods in the Supporting Information), but it is not the most abundant edited transcript in K562 cells. Further testing of differences in editing activity between cells may benefit from overexpression of editing substrates. In an analogous application, dPCR may also be used to accurately measure the abundance of transcripts derived from different alleles having heterozygous single-nucleotide polymorphisms (SNPs), thereby allowing for the assessment of differential allelic imbalance and/or epigenetic silencing across many single cells. Alternatively, analysis of genomic DNA for single-nucleotide variants (SNVs) or copy number variants may be achieved through improved lysis and nucleus digestion, coupled with preamplification.

Our measurements of the BCR-ABL fusion transcript also demonstrate the reliable detection and quantification of rare targets across large numbers of single cells with no false positives observed in no-cell chambers. This sensitivity and specificity may allow for expanding the range of useful single-cell biomarkers, including low-copy transcription factors, and enables the identification and discrimination of minority subpopulations in complex tissues or the detection of rare cells harboring mutations for early detection in the monitoring of minimum residual disease.[40] Although increased dPCR density may be used to extend the current throughput of this device from 200 to approximately 1000 cells per run, practical limitations in fabrication are likely to make further scaling difficult. However, we believe the throughput presented here is well-suited for the analysis and quantification of ultrarare cells, such as circulating tumor cells, following enrichment by fluorescence-activated cell sorting (FACS) or immunocapture.

Integrated single-cell dPCR provides unique capabilities in terms of combined throughput, precision, sensitivity, and specificity.[10,41] These capabilities are complementary to the expanding array of single-cell analysis tools being developed and applied. Here we have demonstrated how these capabilities may be used to measure a variety of transcriptional features, including mRNA expression, miRNA expression, low-copy fusion transcripts, and SNV discrimination. Moving forward, we anticipate that this single-cell platform may be adapted to an expanding range of digital single-cell analyses, including analysis of single-cell copy number variations or aneuploidy, SNV genotyping, and digital protein quantification.[42]

■ ASSOCIATED CONTENT

Supporting Information

Additional information as noted in text. This material is available free of charge via the Internet at http://pubs.acs.org.

■ AUTHOR INFORMATION

Corresponding Author

*E-mail: chansen@phas.ubc.ca. Phone: 604-827-3229. Fax: 604-822-2114.

Author Contributions

A.K.W. and K.A.H. contributed equally to this work. C.L.H. designed the research. A.K.W., K.A.H., C.D., and M.V. designed and fabricated the devices. A.K.W., K.A.H., and C.D. performed the experiments. A.K.W., K.A.H., C.D., and M.V. analyzed the data. A.K.W., K.A.H., and C.L.H. wrote the manuscript.

Notes

The authors declare the following competing financial interests: The technology described in this paper is the subject of a patent filing (PCT/CA2011/000612) that has been licensed to Fluidigm Corp., who provided support for this project. C.L.H. has a financial interest in Fluidigm.

■ ACKNOWLEDGMENTS

This work was supported by the Canadian Institutes of Health Research (CIHR), the Natural Sciences and Engineering Research Council of Canada (NSERC), Fluidigm, Genome BC, and Western Diversification. Salary support for C.L.H. was provided by CIHR and the Michael Smith Foundation for Health Research. A.K.W. was supported by an NSERC Alexander Graham Bell Canada Graduate Doctoral Scholarship.

■ REFERENCES

(1) Murphy, P. J.; Cipriany, B. R.; Wallin, C. B.; Ju, C. Y.; Szeto, K.; Hagarman, J. a; Benitez, J. J.; Craighead, H. G.; Soloway, P. D. *Proc. Natl. Acad. Sci. U.S.A.* **2013**, *110*, 7772−7.

(2) Kantlehner, M.; Kirchner, R.; Hartmann, P.; Ellwart, J. W.; Alunni-Fabbroni, M.; Schumacher, A. *Nucleic Acids Res.* **2011**, *39*, e44.

(3) Tischler, J.; Surani, M. A. *Curr. Opin. Biotechnol.* **2013**, *24*, 69−78.

(4) Taniguchi, Y.; Choi, P. J.; Li, G.-W.; Chen, H.; Babu, M.; Hearn, J.; Emili, A.; Xie, X. S. *Science (New York, N.Y.)* **2010**, *329*, 533−8.

(5) Lecault, V.; Vaninsberghe, M.; Sekulovic, S.; Knapp, D. J. H. F.; Wohrer, S.; Bowden, W.; Viel, F.; McLaughlin, T.; Jarandehei, A.; Miller, M. M.; Falconnet, D.; White, A. K.; Kent, D. G.; Copley, M. R.; Taghipour, F.; Eaves, C. J.; Humphries, R. K.; Piret, J. M.; Hansen, C. L. *Nat. Methods* **2011**, *8*, 581−6.

(6) Falconnet, D.; Niemistö, A.; Taylor, R. J.; Ricicova, M.; Galitski, T.; Shmulevich, I.; Hansen, C. L. *Lab Chip* **2011**, *11*, 466−73.

(7) Yilmaz, O. H.; Kiel, M. J.; Morrison, S. J. *Blood* **2006**, *107*, 924−30.

(8) Notta, F.; Doulatov, S.; Laurenti, E.; Poeppl, A.; Jurisica, I.; Dick, J. E. *Science (New York, N.Y.)* **2011**, *333*, 218−21.

(9) Kent, D. G.; Copley, M. R.; Benz, C.; Wöhrer, S.; Dykstra, B. J.; Ma, E.; Cheyne, J.; Zhao, Y.; Bowie, M. B.; Zhao, Y.; Gasparetto, M.; Delaney, A.; Smith, C.; Marra, M.; Eaves, C. J. *Blood* **2009**, *113*, 6342−50.

(10) White, A. K.; VanInsberghe, M.; Petriv, O. I.; Hamidi, M.; Sikorski, D.; Marra, M. a.; Piret, J.; Aparicio, S.; Hansen, C. L. *Proc. Natl. Acad. Sci. U.S.A.* **2011**, *108*, 13999−4004.

(11) Tang, F.; Lao, K.; Surani, M. A. *Nat. Methods* **2011**, *8*, S6−11.

(12) Ramsköld, D.; Luo, S.; Wang, Y.-C.; Li, R.; Deng, Q.; Faridani, O. R.; Daniels, G. A.; Khrebtukova, I.; Loring, J. F.; Laurent, L. C.; Schroth, G. P.; Sandberg, R. *Nat. Biotechnol.* **2012**, *30*, 777−82.

(13) Bengtsson, M.; Ståhlberg, A.; Rorsman, P.; Kubista, M. *Genome Res.* **2005**, *15*, 1388−92.

(14) Bengtsson, M.; Hemberg, M.; Rorsman, P.; Ståhlberg, A. *BMC Mol. Biol.* **2008**, *9*, 63.

(15) Guo, G.; Huss, M.; Tong, G. Q.; Wang, C.; Li Sun, L.; Clarke, N. D.; Robson, P. *Dev. Cell* **2010**, *18*, 675−85.

(16) Dalerba, P.; Kalisky, T.; Sahoo, D.; Rajendran, P. S.; Rothenberg, M. E.; Leyrat, A. a; Sim, S.; Okamoto, J.; Johnston, D. M.; Qian, D.; Zabala, M.; Bueno, J.; Neff, N. F.; Wang, J.; Shelton, A. a; Visser, B.; Hisamori, S.; Shimono, Y.; Van de Wetering, M.; Clevers, H.; Clarke, M. F.; Quake, S. R. *Nat. Biotechnol.* **2011**, *29*, 1120−1127.

(17) Mestdagh, P.; Feys, T.; Bernard, N.; Guenther, S.; Chen, C.; Speleman, F.; Vandesompele, J. *Nucleic Acids Res.* **2008**, *36*, e143.

(18) Tang, F.; Hajkova, P.; Barton, S. C.; Lao, K.; Surani, M. A. *Nucleic Acids Res.* **2006**, *34*, e9.
(19) Petriv, O. I.; Kuchenbauer, F.; Delaney, a D.; Lecault, V.; White, a; Kent, D.; Marmolejo, L.; Heuser, M.; Berg, T.; Copley, M.; Ruschmann, J.; Sekulovic, S.; Benz, C.; Kuroda, E.; Ho, V.; Antignano, F.; Halim, T.; Giambra, V.; Krystal, G.; Takei, C. J. F.; Weng, a P.; Piret, J.; Eaves, C.; Marra, M. a; Humphries, R. K.; Hansen, C. L. *Proc. Natl. Acad. Sci. U.S.A.* **2010**, *107*, 15443−8.
(20) Diercks, A.; Kostner, H.; Ozinsky, A. *PLoS One* **2009**, *4*, e6326.
(21) Larsson, C.; Grundberg, I.; Söderberg, O.; Nilsson, M. *Nat. Methods* **2010**, *7*, 395−397.
(22) Raj, A.; Van den Bogaard, P.; Rifkin, S. A.; Van Oudenaarden, A.; Tyagi, S. *Nat. Methods* **2008**, *5*, 877−9.
(23) Warren, L.; Bryder, D.; Weissman, I. L.; Quake, S. R. *Proc. Natl. Acad. Sci. U.S.A.* **2006**, *103*, 17807−12.
(24) Lecault, V.; White, A. K.; Singhal, A.; Hansen, C. L. *Curr. Opin. Chem. Biol.* **2012**, *16*, 381−390.
(25) Heyries, K. A.; Tropini, C.; Vaninsberghe, M.; Doolin, C.; Petriv, O. I.; Singhal, A.; Leung, K.; Hughesman, C. B.; Hansen, C. L. *Nat. Methods* **2011**, *8*, 649−51.
(26) Bhat, S.; Herrmann, J.; Armishaw, P.; Corbisier, P.; Emslie, K. R. *Anal. Bioanal. Chem.* **2009**, *394*, 457−67.
(27) Dube, S.; Qin, J.; Ramakrishnan, R. *PLoS One* **2008**, *3*, e2876.
(28) Ling, D.; Salvaterra, P. M. *PLoS One* **2011**, *6*, e17762.
(29) Verma, M.; Karimiani, E. G.; Byers, R. J.; Rehman, S.; Westerhoff, H. V; Day, P. J. R. *Integr. Biol.* **2013**, 543−54.
(30) Sayed, D.; Abdellatif, M. *Physiol. Rev.* **2011**, *91*, 827−87.
(31) Bartel, D. P. *Cell* **2009**, *136*, 215−33.
(32) Pritchard, C. C.; Cheng, H. H.; Tewari, M. *Nat. Rev. Genet.* **2012**, *13*, 358−69.
(33) Christoffersen, N. R.; Silahtaroglu, A.; Orom, U. A.; Kauppinen, S.; Lund, A. H. *RNA (New York, N.Y.)* **2007**, *13*, 1172−8.
(34) Barrey, E.; Saint-Auret, G.; Bonnamy, B.; Damas, D.; Boyer, O.; Gidrol, X. *PLoS One* **2011**, *6*, e20220.
(35) Wu, M.; Piccini, M.; Koh, C.-Y.; Lam, K. S.; Singh, A. K. *PLoS One* **2013**, *8*, e55044.
(36) Shah, S. P.; Morin, R. D.; Khattra, J.; Prentice, L.; Pugh, T.; Burleigh, A.; Delaney, A.; Gelmon, K.; Guliany, R.; Senz, J.; Steidl, C.; Holt, R. A.; Jones, S.; Sun, M.; Leung, G.; Moore, R.; Severson, T.; Taylor, G. A.; Teschendorff, A. E.; Tse, K.; Turashvili, G.; Varhol, R.; Warren, R. L.; Watson, P.; Zhao, Y.; Caldas, C.; Huntsman, D.; Hirst, M.; Marra, M. A.; Aparicio, S. *Nature* **2009**, *461*, 809−13.
(37) Dunham, I.; Kundaje, A.; Aldred, S. F.; Collins, P. J.; Davis, C. A.; Doyle, F.; Epstein, C. B.; Frietze, S.; Harrow, J.; Kaul, R.; Khatun, J.; Lajoie, B. R.; Landt, S. G.; Lee, B.-K.; Pauli, F.; Rosenbloom, K. R.; Sabo, P.; Safi, A.; Sanyal, A.; Shoresh, N.; Simon, J. M.; Song, L.; Trinklein, N. D.; Altshuler, R. C.; Birney, E.; Brown, J. B.; Cheng, C.; Djebali, S.; Dong, X.; Ernst, J.; Furey, T. S.; Gerstein, M.; Giardine, B.; Greven, M.; Hardison, R. C.; Harris, R. S.; Herrero, J.; Hoffman, M. M.; Iyer, S.; Kelllis, M.; Kheradpour, P.; Lassmann, T.; Li, Q.; Lin, X.; Marinov, G. K.; Merkel, A.; Mortazavi, A.; Parker, S. C. J.; Reddy, T. E.; Rozowsky, J.; Schlesinger, F.; Thurman, R. E.; Wang, J.; Ward, L. D.; Whitfield, T. W.; Wilder, S. P.; Wu, W.; Xi, H. S.; Yip, K. Y.; Zhuang, J.; Bernstein, B. E.; Green, E. D.; Gunter, C.; Snyder, M.; Pazin, M. J.; Lowdon, R. F.; Dillon, L. A. L.; Adams, L. B.; Kelly, C. J.; Zhang, J.; Wexler, J. R.; Good, P. J.; Feingold, E. A.; Crawford, G. E.; Dekker, J.; Elinitski, L.; Farnham, P. J.; Giddings, M. C.; Gingeras, T. R.; Guigó, R.; Hubbard, T. J.; Kellis, M.; Kent, W. J.; Lieb, J. D.; Margulies, E. H.; Myers, R. M.; Starnatoyannopoulos, J. A.; Tennebaum, S. A.; Weng, Z.; White, K. P.; Wold, B.; Yu, Y.; Wrobel, J.; Risk, B. A.; Gunawardena, H. P.; Kuiper, H. C.; Maier, C. W.; Xie, L.; Chen, X.; Mikkelsen, T. S.; Gillespie, S.; Goren, A.; Ram, O.; Zhang, X.; Wang, L.; Issner, R.; Coyne, M. J.; Durham, T.; Ku, M.; Truong, T.; Eaton, M. L.; Dobin, A.; Tanzer, A.; Lagarde, J.; Lin, W.; Xue, C.; Williams, B. A.; Zaleski, C.; Röder, M.; Kokocinski, F.; Abdelhamid, R. F.; Alioto, T.; Antoshechkin, I.; Baer, M. T.; Batut, P.; Bell, I.; Bell, K.; Chakrabortty, S.; Chrast, J.; Curado, J.; Derrien, T.; Drenkow, J.; Dumais, E.; Dumais, J.; Duttagupta, R.; Fastuca, M.; Fejes-Toth, K.; Ferreira, P.; Foissac, S.; Fullwood, M. J.; Gao, H.; Gonzalez, D.; Gordon, A.; Howald, C.; Jha, S.; Johnson, R.; Kapranov, P.; King, B.; Kingswood, C.; Li, G.; Luo, O. J.; Park, E.; Preall, J. B.; Presaud, K.; Ribeca, P.; Robyr, D.; Ruan, X.; Sammeth, M.; Sandu, K. S.; Schaeffer, L.; See, L.-H.; Shahab, A.; Skancke, J.; Suzuki, A. M.; Takahashi, H.; Tilgner, H.; Trout, D.; Walters, N.; Wang, H.; Hayashizaki, Y.; Hubbard, T. J.; Reymond, A.; Antonarakis, S. E.; Hannon, G. J.; Ruan, Y.; Carninci, P.; Sloan, C. A.; Learned, K.; Malladi, V. S.; Wong, M. C.; Barber, G. P.; Cline, M. S.; Dreszer, T. R.; Heitner, S. G.; Karolchik, D.; Kirkup, V. M.; Meyer, L. R.; Long, J. C.; Maddren, M.; Raney, B. J.; Grasfeder, L. L.; Giresi, P. G.; Lee, B.-K.; Battenhouse, A.; Sheffield, N. C.; Showers, K. A.; London, D.; Bhinge, A. A.; Shestak, C.; Schaner, M. R.; Kim, S. K.; Zhang, Z. Z.; Mieczkowski, P. A.; Mieczkowska, J. O.; Liu, Z.; McDaniell, R. M.; Ni, Y.; Rashid, N. U.; Kim, M. J.; Adar, S.; Zhang, Z.; Wang, T.; Winter, D.; Keefe, D.; Iyer, V. R.; Sandhu, K. S.; Zheng, M.; Wang, P.; Gertz, J.; Vielmetter, J.; Partridge, E. C.; Varley, K. E.; Gasper, C.; Bansal, A.; Pepke, S.; Jain, P.; Amrhein, H.; Bowling, K. M.; Anaya, M.; Cross, M. K.; Muratet, M. A.; Newberry, K. M.; McCue, K.; Nesmith, A. S.; Fisher-Aylor, K. I.; Pusey, B.; DeSalvo, G.; Parker, S. L.; Balasubramanian, S.; Davis, N. S.; Meadows, S. K.; Eggleston, T.; Newberry, J. S.; Levy, S. E.; Absher, D. M.; Wong, W. H.; Blow, M. J.; Visel, A.; Pennachio, L. A.; Elnitski, L.; Petrykowska, H. M.; Abyzov, A.; Aken, B.; Barrell, D.; Barson, G.; Berry, A.; Bignell, A.; Boychenko, V.; Bussotti, G.; Davidson, C.; Despacio-Reyes, G.; Diekhans, M.; Ezkurdia, I.; Frankish, A.; Gilbert, J.; Gonzalez, J. M.; Griffiths, E.; Harte, R.; Hendrix, D. A.; Hunt, T.; Jungreis, I.; Kay, M.; Khurana, E.; Leng, J.; Lin, M. F.; Loveland, J.; Lu, Z.; Manthravadi, D.; Mariotti, M.; Mudge, J.; Mukherjee, G.; Notredame, C.; Pei, B.; Rodriguez, J. M.; Saunders, G.; Sboner, A.; Searle, S.; Sisu, C.; Snow, C.; Steward, C.; Tapanari, E.; Tress, M. L.; Van Baren, M. J.; Washieti, S.; Wilming, L.; Zadissa, A.; Zhengdong, Z.; Brent, M.; Haussler, D.; Valencia, A.; Raymond, A.; Addleman, N.; Alexander, R. P.; Auerbach, R. K.; Balasubramanian, S.; Bettinger, K.; Bhardwaj, N.; Boyle, A. P.; Cao, A. R.; Cayting, P.; Charos, A.; Cheng, Y.; Eastman, C.; Euskirchen, G.; Fleming, J. D.; Grubert, F.; Habegger, L.; Hariharan, M.; Harmanci, A.; Iyenger, S.; Jin, V. X.; Karczewski, K. J.; Kasowski, M.; Lacroute, P.; Lam, H.; Larnarre-Vincent, N.; Lian, J.; Lindahl-Allen, M.; Min, R.; Miotto, B.; Monahan, H.; Moqtaderi, Z.; Mu, X. J.; O'Geen, H.; Ouyang, Z.; Patacsil, D.; Raha, D.; Ramirez, L.; Reed, B.; Shi, M.; Slifer, T.; Witt, H.; Wu, L.; Xu, X.; Yan, K.-K.; Yang, X.; Zhang, Z.; Struhl, K.; Weissman, S. M.; Tenebaum, S. A.; Penalva, L. O.; Karmakar, S.; Bhanvadia, R. R.; Choudhury, A.; Domanus, M.; Ma, L.; Moran, J.; Victorsen, A.; Auer, T.; Centarin, L.; Eichenlaub, M.; Gruhl, F.; Heerman, S.; Hoeckendorf, B.; Inoue, D.; Kellner, T.; Kirchmaier, S.; Mueller, C.; Reinhardt, R.; Schertel, L.; Schneider, S.; Sinn, R.; Wittbrodt, B.; Wittbrodt, J.; Jain, G.; Balasundaram, G.; Bates, D. L.; Byron, R.; Canfield, T. K.; Diegel, M. J.; Dunn, D.; Ebersol, A. K.; Frum, T.; Garg, K.; Gist, E.; Hansen, R. S.; Boatman, L.; Haugen, E.; Humbert, R.; Johnson, A. K.; Johnson, E. M.; Kutyavin, T. M.; Lee, K.; Lotakis, D.; Maurano, M. T.; Neph, S. J.; Neri, F. V; Nguyen, E. D.; Qu, H.; Reynolds, A. P.; Roach, V.; Rynes, E.; Sanchez, M. E.; Sandstrom, R. S.; Shafer, A. O.; Stergachis, A. B.; Thomas, S.; Vernot, B.; Vierstra, J.; Vong, S.; Wang, H.; Weaver, M. A.; Yan, Y.; Zhang, M.; Akey, J. A.; Bender, M.; Dorschner, M. O.; Groudine, M.; MacCoss, M. J.; Navas, P.; Stamatoyannopoulos, G.; Stamatoyannopoulos, J. A.; Beal, K.; Brazma, A.; Flicek, P.; Johnson, N.; Lukk, M.; Luscombe, N. M.; Sobral, D.; Vaquerizas, J. M.; Batzoglou, S.; Sidow, A.; Hussami, N.; Kyriazopoulou-Panagiotopoulou, S.; Libbrecht, M. W.; Schaub, M. A.; Miller, W.; Bickel, P. J.; Banfai, B.; Boley, N. P.; Huang, H.; Li, J. J.; Noble, W. S.; Bilmes, J. A.; Buske, O. J.; Sahu, A. O.; Kharchenko, P. V; Park, P. J.; Baker, D.; Taylor, J.; Lochovsky, L. *Nature* **2012**, *489*, 57−74.
(38) Warren, L.; Weinstein, J.; Quake, S. R. The Digital Array Response Curve, 2007. http://thebigone.stanford.edu/papers/Weinstein%20DigResCurve.pdf (accessed June 18, 2013).
(39) Faragó, N.; Kocsis, A. K.; Lovas, S.; Molnár, G.; Boldog, E.; Rózsa, M.; Szemenyei, V.; Vámos, E.; Nagy, L. I.; Tamás, G.; Puskás, L. G. *BioTechniques* **2013**, *54*, 327−36.

(40) Kumari, A.; Brendel, C.; Hochhaus, A.; Neubauer, A.; Burchert, A. *Blood* **2012**, *119*, 530−9.
(41) Chen, Y.; Zhang, B.; Feng, H.; Shu, W.; Chen, G. Y.; Zhong, J. F. *Lab Chip* **2012**, *12*, 3930−5.
(42) Ståhlberg, A.; Thomsen, C.; Ruff, D.; Aman, P. *Clin. Chem.* **2012**, *58*, 1682−91.